Physics Letters A 378 (2014) 3457–3463

Contents lists available at ScienceDirect

Physics Letters A

www.elsevier.com/locate/pla

Identification and control of chaos in nonlinear gear dynamic systems using Melnikov analysis

A. Farshidianfar, A. Saghafi *

Mechanical Engineering Department, Ferdowsi University of Mashhad, Mashhad, Iran

ARTICLE INFO

Article history:
Received 28 June 2014
Received in revised form 27 September 2014
Accepted 29 September 2014
Available online 7 October 2014
Communicated by C.R. Doering

Keywords:
Nonlinear dynamics
Gear
Homoclinic bifurcation
Chaos control
Melnikov analysis

ABSTRACT

In this paper, the Melnikov analysis is extended to develop a practical model of gear system to control and eliminate the chaotic behavior. To this end, a nonlinear dynamic model of a spur gear pair with backlash, time-varying stiffness and static transmission error is established. Based on the Melnikov analysis the global homoclinic bifurcation and transition to chaos in this model are predicted. Then non-feedback control method is used to eliminate the chaos by applying an additional control excitation. The regions of the parameter space for the control excitation are obtained analytically. The accuracy of the theoretical predictions and also the performance of the proposed control system are verified by the comparison with the numerical simulations. The simulation results show effectiveness of the proposed control system and present some useful information to analyze and control the gear dynamical systems.

1. Introduction

Gears are widely used in mechanical systems and are known as one of the important sources of noise and vibration. There are many studies on nonlinear dynamics of gear systems and some complicated phenomena such as bifurcation and chaos have been observed. Chaotic behavior is a very interesting nonlinear phenomenon, and it has been detected on some system parameters of a gear system. For instance, Kahraman and Blankenship [1,2] performed some experiments on a spur gear pair and observed several nonlinear phenomena such as sub- and super-harmonic resonances and chaotic behaviors. The Incremental Harmonic Balance method was applied by Raghothama et al. [3] to investigate periodic responses and bifurcations in a nonlinear geared rotor-bearing system. Also, the chaotic response was studied by using numerical integration and the Lyapunov exponent.

Wang et al. [4] analyzed a nonlinear model of gear system associated with friction, backlash and time-varying stiffness. The existence of periodic responses, bifurcation and chaotic motions in system were studied numerically. In [5], Farshidianfar et al. investigated a dynamic model of gear system in which backlash, time-varying stiffness, external excitation and static transmission error were considered. The possibility of existence of homoclinic bifurcation and transition to chaos were studied using Melnikov analysis and numerical simulation method. The results reveal that the system exhibits bifurcation and chaotic motions on some parameters regions. Chang-Jian [6] considered dynamic responses of a gear pair system supported by journal bearings. The possibility of existence of periodic, sub-harmonic and chaotic response for some parameters regions were studied using numerical integration.

From the above mentioned references it can be observed that bifurcation and chaos have been widely found in gear dynamic responses. In order to design and develop an optimal gear transmission system, it is important to predict and control these nonlinear phenomena. Though the previous studies investigated the existence of bifurcation and chaos in gear systems, no heed is paid to the control and elimination of these phenomena.

Chaos control, as an important topic in nonlinear science, has been widely investigated in many science and engineering fields. Hence, feedback and non-feedback control methods have been realized for the control of chaotic systems. Feedback control methods are used to control the chaos by stabilizing a determined unstable periodic orbit which is embedded in a chaotic attractor [7–9], while non-feedback control methods eliminate the chaotic behaviors by applying an additional periodic excitation force or by perturbing a system parameter with small harmonic [10–15]. To control the unstable periodic orbits by feedback methods, the OGY controlling approach being the most representative was introduced by Ott, Grebogi and Yorke [7]. The feedback control methods do not require the information of the system equations, but one must determine the unstable periodic orbits and requires performing

* Corresponding author.
E-mail address: a.i.saghafi@gmail.com (A. Saghafi).

http://dx.doi.org/10.1016/j.physleta.2014.09.060
0375-9601/

several calculations to create the control signal. Hence these methods have some difficulties in practical experiments. In such cases, the non-feedback methods might be more useful and can be easily realized in practical systems. This method requires information of the system equations to create control excitation and does not require continuous tracking of the system state. There are numerous investigations of controlling the chaotic behaviors by applying an additional excitation force or by perturbing a system parameter. For example, Chaon [10] studied suppression of chaos for biharmonically driven dissipative systems. General results concerning suppression of chaos were derived for damped, nonlinear and low-dimensional oscillators subjected to two weak harmonic excitations by using Melnikov method. Wang et al. [13] investigated control of the homoclinic and heteroclinic bifurcations in Duffing equation with two weak forcing excitations by using Melnikov analysis and showed that the chaotic behaviors can be inhibited to periodic orbits. The Melnikov analysis is one of the few analytical methods to study the homoclinic and heteroclinic bifurcations which provides an estimate in the parameter space for the occurrence of chaos in nonlinear system [16]. This method has been widely developed for the analysis of certain dynamical systems [17–24]. In [17] the Melnikov analysis was used to study the chaotic behavior in a nonlinear damped three-well ϕ^6-Van der Pol oscillator under external and parametric excitations. Ravichandran et al. [18] studied the homoclinic bifurcation and transition to the chaos in a nonlinear Duffing oscillator subjected to an amplitude modulated force. Threshold condition for the occurrence of horseshoe chaos was obtained by means of Melnikov method. This analytical method has been extended to study dynamics of the complicated nonlinear systems. Awrejcewicz et al. [19] studied the stick-slip chaos in a four-dimensional self-excited system with Coulomb-like friction. Also, in [20] the Melnikov–Gruendler method was used to predict the stick-slip chaos in double self-excited oscillators. Litak et al. [21] applied the Melnikov method to examine global homoclinic bifurcation and a possible transition to chaos in a double well potential of the Van der Pol system subjected simultaneously to parametric periodic forcing and self-excitation via negative damping term.

In present paper, based on the Melnikov analysis, the non-feedback control method is used to control and eliminate the chaos in gear systems. The paper is organized as follows. In Section 2, a generalized nonlinear model of a spur gear pair is formulated. Also, the Melnikov analysis for defining the existence of the homoclinic bifurcation and chaos is extended. In Section 3, the control model is introduced and the analytical estimates for the control excitation are obtained. Section 4 presents some numerical simulations to validate the theoretical predictions and also to investigate the efficiency of the proposed system to control the homoclinic bifurcation and consequently chaos in nonlinear gear systems. Finally, in Section 5, the conclusions are presented.

2. Description of the model and Melnikov analysis

2.1. Dynamic model formulation

The dynamic model of a spur gear system, investigated in this paper, is shown in Fig. 1 [1–5]. The gear mesh is modeled as a pair of rigid disk connected through a time-varying mesh stiffness $k(t)$, and a constant mesh damping c set along the line of action. In this model, the backlash function f_h, is used to represent gear clearances ($2b$), so the equations of torsional motion can be expressed as [5]:

$$m\frac{d^2\tilde{x}}{dt^2}+c\frac{d\tilde{x}}{dt}+k(t)\,f_h(\tilde{x})=\hat{F}_m+\hat{F}_e(t) \tag{1}$$

where

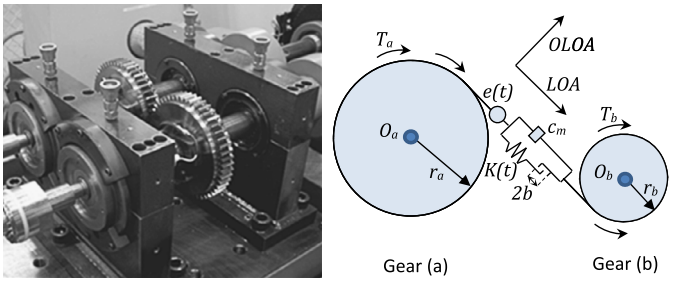

Fig. 1. A spur gear pair model.

$$f_h(\tilde{x})=\begin{cases}\tilde{x}-(1-\alpha)b & b<\tilde{x}\\ \alpha\tilde{x} & -b\le\tilde{x}\le b\\ \tilde{x}+(1-\alpha)b & b<-\tilde{x}\end{cases},\qquad m=\frac{I_aI_b}{I_br_a^2+I_ar_b^2},$$

$$\hat{F}_m=m\left(\frac{T_ar_a}{I_a}+\frac{T_br_b}{I_b}\right),\qquad \hat{F}_e(t)=-m\frac{d^2e(t)}{dt^2}$$

In these equations, I_a and I_b and also r_a and r_b, represent the mass moment of inertia and the base circle radius of the gears (a) and (b). T_a and T_b are the external torques acting on the gears. Additionally, $\tilde{x}(t)$ represents the difference value between the dynamic and static transmission errors and can be written as $\tilde{x}=r_a\theta_a-r_b\theta_b-e$, where θ_a and θ_b are the torsional displacements of the gears. The static transmission error $e(t)$ is also applied at the gear mesh interface to represent any manufacturing errors and teeth deformations from perfect involute form. The static transmission error is a periodic function, its fundamental frequency is the meshing frequency [25]. Moreover, the mesh stiffness of the gear is a periodic function depending on the number and position of the teeth in contact. So, the static transmission error and the mesh stiffness can be expressed as a harmonic function with $e(t)=e(t+2\pi/\omega_e)=e\cos(\omega_et+\phi_e)$ and $k(t)=k(t+2\pi/\omega_k)=k_m+k_p\cos(\omega_kt+\phi_k)$, respectively. By defining

$$x=\tilde{x}/b,\qquad \omega_n=\sqrt{k_m/m},\qquad \tau=\omega_nt,\qquad \Omega_k=\omega_k/\omega_n,$$
$$\Omega_e=\omega_e/\omega_n,\qquad \tilde{\mu}=c/2m\omega_n,\qquad \tilde{k}_p=k_p/m\omega_n^2,$$
$$\tilde{F}_m=\hat{F}_m/bk_m,\qquad \tilde{F}_e=e/b$$

The dimensionless form of Eq. (1) can be written as

$$\frac{d^2x}{d\tau^2}+2\tilde{\mu}\frac{dx}{d\tau}+\left(1+\tilde{k}_p\cos(\Omega_k\tau+\phi_k)\right)f_h(x)=\tilde{F}_m+\tilde{F}_e\Omega_e^2\cos(\Omega_e\tau+\phi_e) \tag{2}$$

where

$$f_h(x)=\begin{cases}x-(1-\alpha) & 1<x\\ \alpha x & -1\le x\le 1\\ x+(1-\alpha) & 1<-x\end{cases}$$

The backlash function is a stepwise linear function and a 3-order approximation polynomial is suggested to express it. For the particular case of $\alpha=0$, the approximated function can be expressed as, $f_h(x)=-0.1667x+0.1667x^3$. Thus, the equation of motion is given by:

$$\frac{d^2x}{d\tau^2}+2\tilde{\mu}\frac{dx}{d\tau}+\left(1+\tilde{k}_p\cos(\Omega_k\tau+\phi_k)\right)\left(-0.1667x+0.1667x^3\right)=\tilde{F}_m+\tilde{F}_e\Omega_e^2\cos(\Omega_e\tau+\phi_e) \tag{3}$$

In the following, the prediction and control of chaotic behavior for this equation will be investigated.

2.2. Melnikov analysis and chaos prediction

Study of global homoclinic bifurcation that provides the estimate for the occurrence of chaotic behavior in some nonlinear systems is well done by the Melnikov analysis. The occurrence of transverse intersection of the perturbed stable and unstable manifolds of the homoclinic orbits are called homoclinic bifurcation and defined as a criterion for prediction of onset of the chaos. The Melnikov method measures the distance between the stable and unstable manifolds of the perturbed system in the Poincare section, and provides an analytical estimate for the occurrence of homoclinic bifurcation and hence transition to chaos [16].

In order to apply the Melnikov analysis, the average force, the excitation term, the mesh stiffness and also the damping term are considered as small perturbations to the Hamiltonian system. Thus, considering ε as a small parameter and scaling $\tilde{F}_m = \varepsilon f_m$, $\tilde{F}_e = \varepsilon f_e$, $\tilde{k}_p = \varepsilon k_p$ and $\tilde{\mu} = \varepsilon \mu$, the generalized Eq. (3) can be rewritten in the vector form as:

$$\dot{X} = W_o(X) + \varepsilon W_p(X, \tau) \tag{4}$$

where $X = (x, y = dx/d\tau)$ is the state vector, W_o and W_p represents the vector field and the perturbed vector, and are given by

$$\begin{aligned} W_o(X) &= \left(y, ax - cx^3\right) \\ W_p(X, \tau) &= (0, -2\mu\dot{x} + k_p \cos(\Omega_k \tau + \phi_k)\left(ax - cx^3\right) + f_m \\ &\quad + \Omega_e^2 f_e \cos(\Omega_e \tau + \phi_e) \end{aligned} \tag{5}$$

where $a = c = 0.1667$. For the unperturbed system, when $\varepsilon = 0$, the system is a planar Hamiltonian system with a Hamiltonian function as $H(x, y) = \frac{1}{2}y^2 - \frac{a}{2}x^2 + \frac{c}{4}x^4$. For $\varepsilon = 0$ this system has two centers at $(\pm\sqrt{(a/c)}, 0)$ and a hyperbolic saddle at $(0, 0)$. The saddle point is connected to itself by two homoclinic orbits with the expressions

$$\begin{aligned} X_h &= \left(x_h(\bar{\tau}), y_h(\bar{\tau})\right) \\ &= \left(\pm\sqrt{\frac{2a}{c}}\operatorname{sech}\left(\sqrt{a}(\bar{\tau})\right), \mp\sqrt{\frac{2}{c}}a\operatorname{sech}\left(\sqrt{a}(\bar{\tau})\right)\tanh\left(\sqrt{a}(\bar{\tau})\right)\right) \end{aligned} \tag{6}$$

where $\tau - \tau_0 = \bar{\tau}$. The Hamiltonian function and also the stable and unstable manifolds of the homoclinic orbits ($W_s^{\pm}$ and $W_u^{\pm}$), for the unperturbed system are shown in Fig. 2. The Melnikov function of system (5) is given as follows [5]:

$$\begin{aligned} M(\tau_0) &= \int_{-\infty}^{+\infty} y_h(\tau)\left(-2\mu y_h(\tau) + k_p \cos\left(\Omega_k(\tau + \tau_0) + \phi_k\right)\right. \\ &\quad \times \left(ax_h(\tau) - cx_h(\tau)^3\right) + f_m \\ &\quad \left. + \Omega_e^2 f_e \cos\left(\Omega_e(\tau + \tau_0) + \phi_e\right)\right) d\tau \\ \Rightarrow M(\tau_0) &= \int_{-\infty}^{+\infty} \left(\mp\sqrt{\frac{2}{c}}a\operatorname{sech}(\sqrt{a}\tau)\tanh(\sqrt{a}\tau)\right) \\ &\quad \times \left(-2\mu\left(\mp\sqrt{\frac{2}{c}}a\operatorname{sech}(\sqrt{a}\tau)\tanh(\sqrt{a}\tau)\right)\right. \\ &\quad + k_p \cos\left(\Omega_k(\tau + \tau_0) + \phi_k\right)\left(a\left(\pm\sqrt{\frac{2a}{c}}\operatorname{sech}(\sqrt{a}\tau)\right)\right. \\ &\quad \left.\left. - c\left(\pm\sqrt{\frac{2a}{c}}\operatorname{sech}(\sqrt{a}\tau)\right)^3\right) + f_m \right. \\ &\quad \left. + f_e\Omega_e^2 \cos\left(\Omega_e(\tau + \tau_0) + \phi_e\right)\right) d\tau \end{aligned} \tag{7}$$

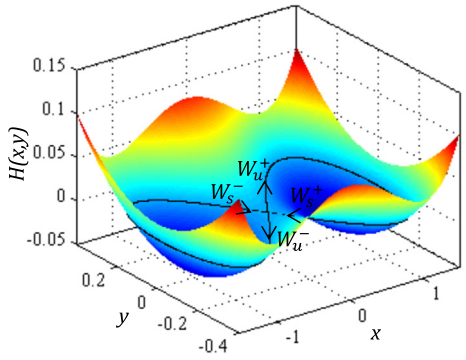

Fig. 2. Hamiltonian function and also the stable and unstable manifolds of the homoclinic orbits.

After integration, the Melnikov function is obtained as

$$\begin{aligned} M^{\pm}(\tau_0) &= -\frac{8}{3}\frac{\mu(a)^2}{c\sqrt{a}} + \left(\frac{a}{c} - \frac{1}{6c}\left(4a + \Omega_k^2\right)\right)k_p\Omega_k^2\pi \\ &\quad \times \operatorname{csch}\left(\frac{\pi\Omega_k}{2\sqrt{a}}\right)\sin(\Omega_k\tau_0 + \phi_k) \\ &\quad \pm\sqrt{\frac{2}{c}}f_e\Omega_e^3\pi\operatorname{sech}\left(\frac{\pi\Omega_e}{2\sqrt{a}}\right)\sin(\Omega_e\tau_0 + \phi_e) \end{aligned} \tag{8}$$

Using the Melnikov theorem if $M(\tau_0)$ has a simple zero, then the manifolds intersect transversally. Transverse intersection of these manifolds provide an estimate in the parameter space for the occurrence of homoclinic bifurcation and hence transition to chaos. Design and proper choice of system parameters is the basic idea for suppression or elimination of the chaotic behavior [5]. It should be noted that there are limitations on the design and choice of some system parameters. Therefore, the values of control parameters are available only to a specific region and based on engineering justification. In such conditions the methods of controlling chaos are proposed.

3. Control system description

In this section, based on Melnikov theory, a practical non-feedback controller is suggested such that one can control and eliminate the chaotic responses of a gear system. To this end, the gear body and corresponding shaft are connected via several actuators for one set of gear–shaft coupling to apply an additional control excitation to the driver gear, as shown in Fig. 3 (see also [26]). These actuators can transmit the mean torque and simultaneously generate additional excitation $U_p(t)$ to control the chaos. The additional control excitation is considered as harmonic with $U_p(t) = U_p\cos(\omega_p t + \phi_p)$, and the Melnikov analysis is extended to obtain an analytical estimate of the suitable parameter spaces for this control excitation term [10–15]. The dynamic equation of this model, including the $U_p(t)$, is obtained as [5]:

$$m\frac{d^2\tilde{x}}{dt^2} + c\frac{d\tilde{x}}{dt} + k(t)f_h(\tilde{x}) = \hat{F}_m + \hat{F}_e(t) + \hat{F}_p\cos(\omega_p t + \phi_p) \tag{9}$$

where $\hat{F}_p = m(r_a/I_a)U_p$. By defining the dimensionless excitation frequency and amplitude as $\Omega_p = \omega_p/\omega_n$, $\tilde{F}_p = \hat{F}_p/bk_m$ and also considering the dimensionless parameters, defined in Eq. (2), the following equation is yielded.

$$\begin{aligned} &\frac{d^2x}{d\tau^2} + 2\tilde{\mu}\frac{dx}{d\tau} + \left(1 + \tilde{k}_p\cos(\Omega_k\tau + \phi_k)\right)f_h(x) \\ &\quad = \tilde{F}_m + \tilde{F}_e\Omega_e^2\cos(\Omega_e\tau + \phi_e) + \tilde{F}_p\cos(\Omega_p\tau + \phi_p) \end{aligned} \tag{10}$$

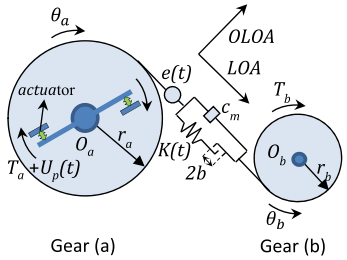

Fig. 3. The gear control model including the additional excitation term.

The results of previous section are applied for system equation (10). Also, suppose that the amplitude of excitation term is a weak perturbations as $\tilde{F}_p = \varepsilon f_p$, then the Melnikov function for this model is obtained as:

$$M(\tau_0) = \int_{-\infty}^{+\infty} \left(\mp\sqrt{\frac{2}{c}} a \operatorname{sech}(\sqrt{a}\tau) \tanh(\sqrt{a}\tau) \right) \times \left(-2\mu \left(\mp\sqrt{\frac{2}{c}} a \operatorname{sech}(\sqrt{a}\tau) \tanh(\sqrt{a}\tau) \right) + k_p \cos\big(\Omega_k(\tau+\tau_0)+\phi_k\big) \left(a \left(\pm\sqrt{\frac{2a}{c}} \operatorname{sech}(\sqrt{a}\tau) \right) - c \left(\pm\sqrt{\frac{2a}{c}} \operatorname{sech}(\sqrt{a}\tau) \right)^3 \right) + f_m + f_e \Omega_e^2 \cos\big(\Omega_e(\tau+\tau_0)+\phi_e\big) + f_p \cos\big(\Omega_p(\tau+\tau_0)+\phi_p\big) \right) d\tau \quad (11)$$

The fundamental frequency of the static transmission error and the mesh stiffness is the meshing frequency. Therefore, the dimensionless frequencies Ω_k and Ω_e are equal and can be considered as $\Omega_k = \Omega_e = \Omega$. Also, there is a phase difference between the static transmission error and the mesh stiffness as $\phi_k = \phi_e + \pi$. Hence, the Melnikov function (11) can be simplifies to

$$M^{\pm}(\tau_0) = A + (B \pm E)\sin(\Omega\tau_0 + \phi_e) \pm P \sin(\Omega_p\tau_0 + \phi_p) \quad (12)$$

with

$$A = -\frac{8}{3}\frac{\mu(a)^2}{c\sqrt{a}},$$

$$B = \left(\frac{1}{6c}\big(4a+\Omega^2\big) - \frac{a}{c}\right) k_p \Omega^2 \pi \operatorname{csch}\left(\frac{\pi\Omega}{2\sqrt{a}}\right),$$

$$E = \sqrt{\frac{2}{c}} f_e \Omega^3 \pi \operatorname{sech}\left(\frac{\pi\Omega}{2\sqrt{a}}\right),$$

$$P = \sqrt{\frac{2}{c}} f_p \Omega_p \pi \operatorname{sech}\left(\frac{\pi\Omega_p}{2\sqrt{a}}\right)$$

Comparing Eq. (12) with the Melnikov function given by Eq. (8), it is concluded that the control excitation term $\pm\sqrt{\frac{2}{c}} f_p \Omega_p \pi \times \operatorname{sech}(\frac{\pi\Omega_p}{2\sqrt{a}}) \sin(\Omega_p\tau_0 + \phi_p)$ adds to the Melnikov function. According to the Melnikov function (8), in the absence of control excitation, transverse intersections of the stable and unstable manifolds $W_s^{\pm}$ and $W_u^{\pm}$ occurs for certain parameter values which satisfy the relation

$$|A| < |B \pm E| \Rightarrow \left| -\frac{8}{3}\frac{\mu(a)^2}{c\sqrt{a}} \right| < \left| \left(\frac{1}{6c}\big(4a+\Omega^2\big) - \frac{a}{c}\right) k_p \Omega^2 \pi \operatorname{csch}\left(\frac{\pi\Omega}{2\sqrt{a}}\right) \pm \sqrt{\frac{2}{c}} f_e \Omega^3 \pi \operatorname{sech}\left(\frac{\pi\Omega}{2\sqrt{a}}\right) \right| \quad (13)$$

Now, the additional excitation is added on the chaotic system. In this case, a necessary condition for $M^{\pm}$ to be same sign for all τ_0 is [10]:

$$|P| > |B \pm E| - |A| = P_{\min}$$

$$\left| \sqrt{\frac{2}{c}} f_p \Omega_p \pi \operatorname{sech}\left(\frac{\pi\Omega_p}{2\sqrt{a}}\right) \right| > \left| \left(\frac{1}{6c}\big(4a+\Omega^2\big) - \frac{a}{c}\right) k_p \Omega^2 \pi \operatorname{csch}\left(\frac{\pi\Omega}{2\sqrt{a}}\right) \pm \sqrt{\frac{2}{c}} f_e \Omega^3 \pi \operatorname{sech}\left(\frac{\pi\Omega}{2\sqrt{a}}\right) \right| - \left| -\frac{8}{3}\frac{\mu(a)^2}{c\sqrt{a}} \right| \quad (14)$$

The optimal values of excitation phase ($\phi_p = \phi_{optimum}$), which corresponds to the widest amplitude ranges for the chaos elimination, are obtained for the situation in which the maximum (maximum for A < 0 and minimum for A > 0) of $A + (B \pm E)\sin(\Omega\tau_0 + \phi_e)$ and $\mp P_{\min}\sin(\Omega_p\tau_0 + \phi_{optimum})$ occur at the same τ_0. $(B+E)$ and P (for M^-: $(B-E)$ and $(-P)$) will be considered to be same sign. It is clear that changing this sign is the equivalent of shifting the phase as $\phi_e \to \tilde{\phi}_e + \pi$. Also, in this gear dynamic model, the dimensionless excitation frequency Ω_p is assumed as $\Omega_p = \Omega_e = \Omega$. Thus, $\phi_{optimum} = \pi + \phi_e$ is obtained for the optimal value of excitation phase. Moreover, for this optimal excitation phase the upper threshold value of excitation amplitude can be obtained as

$$P_{\max} = \left| \left(\frac{1}{6c}\big(4a+\Omega^2\big) - \frac{a}{c}\right) k_p \Omega^2 \pi \operatorname{csch}\left(\frac{\pi\Omega}{2\sqrt{a}}\right) \pm \sqrt{\frac{2}{c}} f_e \Omega^3 \pi \operatorname{sech}\left(\frac{\pi\Omega}{2\sqrt{a}}\right) \right| + \left| -\frac{8}{3}\frac{\mu(a)^2}{c\sqrt{a}} \right| \quad (15)$$

Also, the Melnikov functions indicated that the excitation phase can be changed in suitable interval as $[\phi_{optimum} - \Delta\phi_{\max}, \phi_{optimum} + \Delta\phi_{\max}]$. Where, $\Delta\phi_{\max}$ is the maximum deviation of excitation phase from $\phi_{optimum}$. The maximum deviation of excitation phase $\Delta\phi_{\max}$ can be obtained based on the nearest zeros of $A + (B \pm E)\sin(\Omega\tau_0 + \phi_e)$ and $\pm P\sin(\Omega_p\tau_0 + \phi_{optimum})$, and are given by:

$$\Delta\phi_{\max} = \Omega_p\big(\tau_0^2 - \tau_0^1\big) = \arcsin\frac{A}{(B \pm E)} \quad (16)$$

Where, τ_0^1 and τ_0^2 presents the nearest zeros of $\pm P\sin(\Omega_p\tau_0 + \phi_{optimum})$ and $A + (B \pm E)\sin(\Omega\tau_0 + \phi_e)$, respectively. For an arbitrary deviation of $\Delta\phi$ $(0 < \Delta\phi < \Delta\phi_{\max})$ from $\phi_{optimum}$ one can easily obtain the allowed amplitude value of $P_{\max}$ ($< P_{\max}$ at $\phi_{optimum}$), and $P_{\min}$ ($> P_{\min}$ at $\phi_{optimum}$), for which $M^{\pm}$ to be same sign. Therefore, there exist suitable intervals of excitation amplitude and phase for elimination of chaos in this dynamic model.

4. Numerical simulation

To validate the accuracy of the proposed analytical predictions and also to investigate the efficiency of the proposed control system, the numerical simulation is done. As mentioned in Section 3, Eq. (8) presents the Melnikov function of system in the absence of chaos elimination excitation. Using this equation and choosing f_e as the control parameter, the threshold values for transverse intersection of the stable and unstable manifolds and hence the occurrence of the homoclinic bifurcation are predicted as:

For W^+:

$$f_{e(1)} = \left(\left(\frac{a}{c} - \frac{1}{6c}(4a+\Omega^2)\right)k_p\Omega^2\pi\ \mathrm{csch}\left(\frac{\pi\Omega}{2\sqrt{a}}\right) + \left|-\frac{8}{3}\frac{\mu(a)^2}{c\sqrt{a}}\right|\right)\Big/\left(\sqrt{\frac{2}{c}}\Omega^3\pi\ \mathrm{sech}\left(\frac{\pi\Omega}{2\sqrt{a}}\right)\right) \quad (17a)$$

or:

$$f_{e(2)} = \left(\left(\frac{a}{c} - \frac{1}{6c}(4a+\Omega^2)\right)k_p\Omega^2\pi\ \mathrm{csch}\left(\frac{\pi\Omega}{2\sqrt{a}}\right) - \left|-\frac{8}{3}\frac{\mu(a)^2}{c\sqrt{a}}\right|\right)\Big/\left(\sqrt{\frac{2}{c}}\Omega^3\pi\ \mathrm{sech}\left(\frac{\pi\Omega}{2\sqrt{a}}\right)\right) \quad (17b)$$

For W^-:

$$f_{e(3)} = \left(\left(-\frac{a}{c} + \frac{1}{6c}(4a+\Omega^2)\right)k_p\Omega^2\pi\ \mathrm{csch}\left(\frac{\pi\Omega}{2\sqrt{a}}\right) - \left|-\frac{8}{3}\frac{\mu(a)^2}{c\sqrt{a}}\right|\right)\Big/\left(\sqrt{\frac{2}{c}}\Omega^3\pi\ \mathrm{sech}\left(\frac{\pi\Omega}{2\sqrt{a}}\right)\right) \quad (17c)$$

or:

$$f_{e(4)} = \left(\left(-\frac{a}{c} + \frac{1}{6c}(4a+\Omega^2)\right)k_p\Omega^2\pi\ \mathrm{csch}\left(\frac{\pi\Omega}{2\sqrt{a}}\right) + \left|-\frac{8}{3}\frac{\mu(a)^2}{c\sqrt{a}}\right|\right)\Big/\left(\sqrt{\frac{2}{c}}\Omega^3\pi\ \mathrm{sech}\left(\frac{\pi\Omega}{2\sqrt{a}}\right)\right) \quad (17d)$$

Thus, in this system the chaos may appear for certain parameter values which satisfy the relation

$$\text{for } W^+\text{: } f_e > f_{e(1)} \text{ or } f_e < f_{e(2)} \quad \text{and}$$
$$\text{for } W^-\text{: } f_e < f_{e(3)} \text{ or } f_e > f_{e(4)} \quad (18)$$

The Melnikov critical values of f_e (f_{e1}, f_{e2}, f_{e3} and f_{e4}) for homoclinic bifurcation as functions of frequency Ω, at $\mu = 7$ and $k_p = 5$ are shown in Fig. 4. In the parameter regions above the threshold curve f_{e1} and below the threshold curve f_{e2}, M^+ change its sign. As a result, in these regions transverse intersection of the stable and unstable manifolds W_s^+ and W_u^+ occurs, so existence of chaos is expected. Also, in the regions below the threshold curve f_{e3}, and above the threshold curve f_{e4}, M^- changes its sign, transverse intersection of the manifolds W_s^- and W_u^- occur.

To demonstrate the accuracy of the analytical predictions, the numerical simulation of Eq. (3) is done. Fig. 5 shows the bifurcation diagram with varying the internal excitation term $\tilde{F}_e$ ($\tilde{F}_e = \varepsilon f_e$) from -0.35 to 0.35. The values of the other parameters are assumed as $\Omega = 0.5$, $f_m = 1$, $\mu = 7$, $k_p = 5$, $\varepsilon = 0.01$ and initial conditions as $x = 0.01$ and $\dot{x} = 0.01$. It can be seen that the period doubling bifurcation and also transition to chaos occurs at $\tilde{F}_e < -0.2$, and $\tilde{F}_e > 0.21$. Using Eq. (18) (see also Fig. 4) the critical parameter values of f_e for transverse intersection of the homoclinic orbits, and specially when $\Omega = 0.5$, are obtained at $f_{e1} = 19.83$, $f_{e2} = -19.33$, $f_{e3} = -19.83$, and $f_{e4} = 19.33$. So, the numerical results are in good agreement with the theoretical predictions and confirm the analysis.

To analyze controlling the chaotic responses, the system at $f_e = 25$, $\Omega = 0.5$, $f_m = 1$, $\mu = 7$, and $k_p = 5$ is considered. It can be observed that these parameters correspond to the point situated above the threshold values f_{e1} and f_{e4}, and thus, chaotic motion occurs (see Figs. 4 and 5).

To apply the above control approach, a suitable control excitation $U_p(t)$ is added to the chaotic system. At $f_e = 25$, using Eqs. (14) and (15), the lower and upper threshold values of excitation amplitude are obtained as:

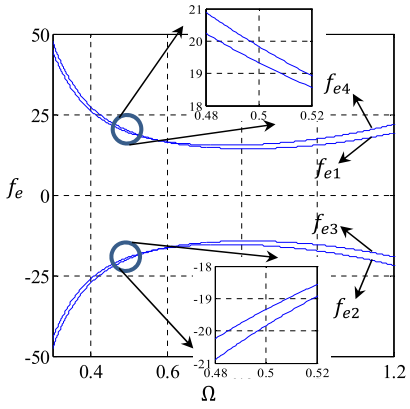

Fig. 4. Threshold curves for homoclinic bifurcation in the $(f_e - \Omega)$ plane at $\mu = 7$ and $k_p = 5$.

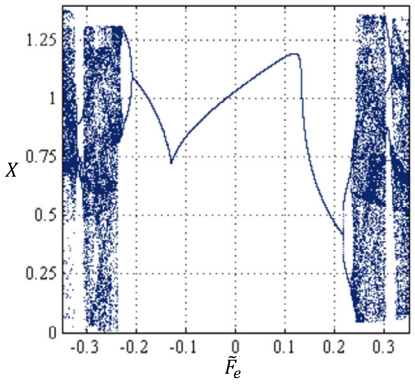

Fig. 5. Bifurcation diagram for control parameter $\tilde{F}_e$ ($\tilde{F}_e = \varepsilon f_e$).

$$\text{for } M^+\text{: } P_{\min} = 2.008 \Rightarrow f_{p(\min)} = 1.29 \quad \text{and}$$
$$\text{for } M^-\text{: } P_{\min} = 2.203 \Rightarrow f_{p(\min)} = 1.42$$
$$\text{for } M^+\text{: } P_{\max} = 17.251 \Rightarrow f_{p(\max)} = 11.08 \quad \text{and}$$
$$\text{for } M^-\text{: } P_{\max} = 17.446 \Rightarrow f_{p(\max)} = 11.21 \quad (19)$$

Thus, the maximum theoretical interval of excitation amplitude for both $M^{\pm}(\tau_0)$ is now $f_p = [1.42\ 11.08]$. By using Eq. (16), $\Delta\phi_{\max} = 0.9132$ and 0.8879 are given for the maximum deviation of excitation phase from $\phi_{optimum}$ for M^+ and M^-, respectively. Thus, the maximum allowed interval of excitation phase is approximately $\phi_p = [\pi + \phi_e - 0.8879\ \ \pi + \phi_e + 0.8879]$. For each value of ϕ_p belonging to such interval, certain suitable amplitude exists. The suitable amplitude and phase intervals for the control excitation term are shown in Fig. 6. For instance, at $\phi_p = \phi_{optimum} = \pi + \phi_e$, which corresponds to the widest amplitude interval for the control excitation, the bifurcation diagram is plotted. Fig. 7 presents the bifurcation diagram of system for control parameter $\tilde{F}_p = \varepsilon f_p$ at $\Omega = \Omega_p = 0.5$, $f_m = 1$, $\mu = 7$, $k_p = 5$, $\phi_e = 0$, $\varepsilon = 0.01$ and $\phi_p = \pi$. From this figure, the numerically interval of chaos elimination is [0.01 0.115] and confirm the theoretical predictions. The bifurcation diagram of system for control parameter ϕ_p at $\Omega = \Omega_p = 0.5$, $f_m = 1$, $\mu = 7$, $k_p = 5$, $\phi_e = 0$, $\varepsilon = 0.01$ and $f_p = 4$, is shown in Fig. 8. The theoretical interval of ϕ_p is now [2.25 4.03], and the numerical results show the chaos elimination interval as [2.15 4.18].

Also, the bifurcation diagram for control parameter $\tilde{F}_p = \varepsilon f_p$ at $\phi_p = \pi + 0.5$ and $\phi_e = 0$ is shown in Fig. 9. According to this figure, the numerically interval of chaos elimination is [0.012 0.098], which is in good agreement with the theoretical predictions. By applying the additional control excitation belonging to this interval, chaotic motion can be eliminate. Figs. 10–12 demonstrate controlling the chaotic behavior for the control excitation parameters

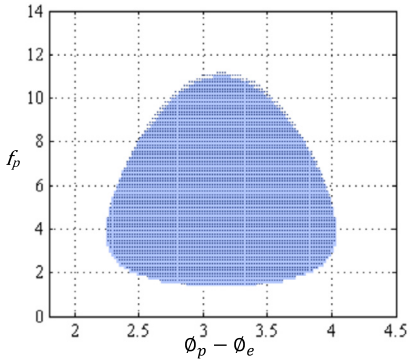

Fig. 6. The suitable amplitude and phase intervals of control excitation for M^+ (blue space) and for M^- (dotted space). (For interpretation of the references to color in this figure legend, the reader is referred to the web version of this article.)

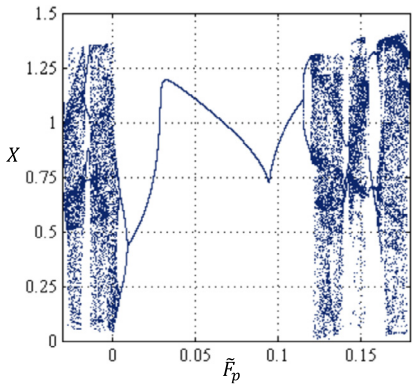

Fig. 7. Bifurcation diagram for control parameter $\tilde{F}_p$ at $\phi_p = \pi$.

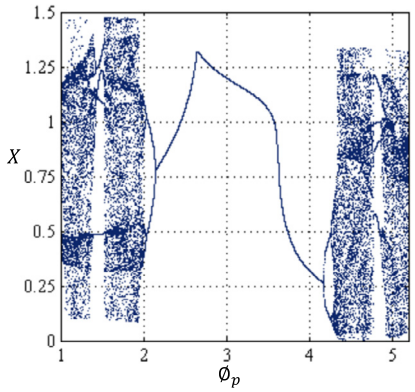

Fig. 8. Bifurcation diagram for control parameter ϕ_p at $f_p = 4$.

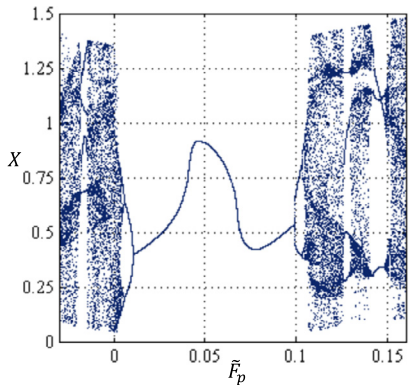

Fig. 9. Bifurcation diagram for control parameter $\tilde{F}_p$ at $\phi_p = \pi + 0.5$.

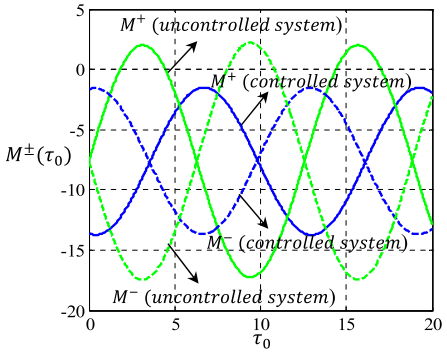

Fig. 10. The Melnikov function for uncontrolled (green) and controlled (blue) system. (For interpretation of the references to color in this figure legend, the reader is referred to the web version of this article.)

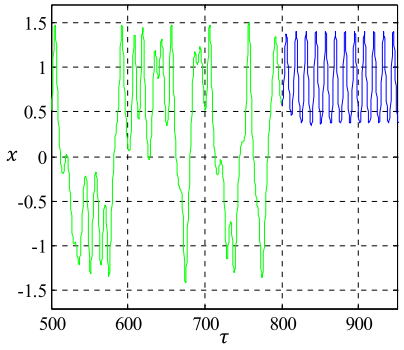

Fig. 11. The time response for uncontrolled (green) and controlled (blue) system. (For interpretation of the references to color in this figure legend, the reader is referred to the web version of this article.)

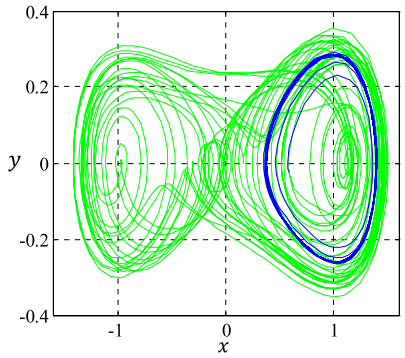

Fig. 12. The phase portrait for uncontrolled (green) and controlled (blue) system. (For interpretation of the references to color in this figure legend, the reader is referred to the web version of this article.)

$f_p = 8$, $\phi_p = \pi + 0.5$. Fig. 10 shows the Melnikov function for this point. After the additional excitation is added on the system, the Melnikov functions do not change sign, thus elimination of chaos is expected.

The time history of this point for $U_p = 0$ in the range $\tau =$ [0 800] is given in Fig. 11, while the corresponding phase portrait is given in Fig. 12, respectively. The chaotic response of the system are clearly visible in these figures (Figs. 11 and 12, green line), which are in agreement with the results obtained in Figs. 4 and 5. Now, the control excitation is applied at $\tau \geq 800$. The simulation results are illustrated in Figs. 11 and 12 (blue line). In these figures, it can be seen that the chaos are vanished and finally a periodic responses achieved. Simulation results confirm the theoretical predictions and show effectiveness of the proposed control system to

elimination and control of the homoclinic bifurcation and chaos in nonlinear gear systems.

5. Conclusion

This paper has discussed a control system to inhibition the chaotic responses of gears system. The Melnikov analytical analysis has been used to derive analytical prediction for the occurrence of homoclinic bifurcation and transition to the chaotic behaviors. Then chaos control of this gear system has been carried out using a non-feedback control strategy by applying an additional control excitation. A generalized nonlinear model of a spur gear pair has been developed to investigate the required control excitation. The accuracy of the theoretical predictions, and also the performance of the proposed control system have been validated with the numerical simulations. The results of the analysis indicate the efficiency and also feasibility of this control method, and consequently this control concept can be proposed as a way of implementing the chaos control in gear transmission system.

References

[1] G.W. Blankenship, A. Kahraman, A steady state forced response of a mechanical oscillator with combined parametric excitation and clearance type nonlinearity, J. Sound Vib. 185 (5) (1995) 743–765.

[2] A. Kahraman, G.W. Blankenship, Experiments on nonlinear dynamic behavior of an oscillator with clearance and periodically time-varying parameters, J. Appl. Mech. 64 (1997) 217–226.

[3] A. Raghothama, S. Narayanan, Bifurcation and chaos in geared rotor bearing system by incremental harmonic balance method, J. Sound Vib. 226 (3) (1999) 469–475.

[4] J. Wang, J. Zheng, A. Yang, An analytical study of bifurcation and chaos in a spur gear pair with sliding friction, Proc. Eng. 31 (2012) 563–570.

[5] A. Farshidianfar, A. Saghafi, Global bifurcation and chaos analysis in nonlinear vibration of spur gear systems, Nonlinear Dyn. 75 (2014) 783–806.

[6] C.W. Chang-Jian, Strong nonlinearity analysis for gear-bearing system under nonlinear suspension bifurcation and chaos, Nonlinear Anal., Real World Appl. 11 (2010) 1760–1774.

[7] E. Ott, N. Grebogi, J. Yorke, Controlling chaos, Phys. Rev. Lett. 64 (11) (1990) 1196–1199.

[8] F.N. Koumboulis, B.G. Mertzios, Feedback controlling against chaos, Chaos Solitons Fractals 11 (2000) 351–358.

[9] A. Uchida, S. Kinugawa, S. Yoshimori, Synchronization of chaos in two microchip lasers by using incoherent feedback method, Chaos Solitons Fractals 17 (2003) 363–368.

[10] R. Chacon, General results on chaos suppression for biharmonically driven dissipative systems, Phys. Lett. A 257 (1999) 293–300.

[11] M. Belhaq, M. Houssni, Suppression of chaos in averaged oscillator driven by external and parametric excitations, Chaos Solitons Fractals 11 (2000) 1237–1246.

[12] R. Chacon, Role of ultrasubharmonic resonances in taming chaos by weak harmonic perturbations, Europhys. Lett. 54 (2) (2001) 148–153.

[13] R. Wang, J. Deng, Z. Jing, Chaos control in duffing system, Chaos Solitons Fractals 27 (2006) 249–257.

[14] J. Yang, Z. Jing, Controlling chaos in a pendulum equation with ultra-subharmonic resonances, Chaos Solitons Fractals 42 (2009) 1214–1226.

[15] R. Chacon, A.M. Lacasta, Controlling chaotic transport in two-dimensional periodic potentials, Phys. Rev. E 82 (2010) 046207.

[16] J. Guckenheimer, P. Holmes, Nonlinear Oscillations, Dynamical Systems, and Bifurcations of Vector Fields, Springer, New York, 1983.

[17] M. Siewe Siewe, F.M. Moukam Kakmeni, C. Tchawoua, P. Woafo, Bifurcations and chaos in the triple-well ϕ^6 Van der Pol oscillator driven by external and parametric excitations, Physica A 357 (2005) 383–396.

[18] V. Ravichandran, V. Chinnathambi, S. Rajasekar, Homoclinic bifurcation and chaos in Duffing oscillator driven by an amplitude-modulated force, Physica A 376 (2007) 223–236.

[19] J. Awrejcewicz, D. Sendkowski, How to predict stick-slip chaos in R^4, Phys. Lett. A 330 (2004) 371–376.

[20] J. Awrejcewicz, M. Holicke, Analytical prediction of stick-slip chaos in a double self-excited Duffing-type oscillator, Math. Probl. Eng. (2006) 1–79, http://dx.doi.org/10.1155/MPE/2006/70245.

[21] G. Litak, M. Borowiec, A. Syta, K. Szabelski, Transition to chaos in the self-excited system with a cubic double well potential and parametric forcing, Chaos Solitons Fractals 40 (2009) 2414–2429.

[22] J. Awrejcewicz, Y. Pyryev, Chaos prediction in the duffing-type system with friction using Melnikov's function, Nonlinear Anal., Real World Appl. 7 (2006) 12–24.

[23] K. Yagasaki, Bifurcations and chaos in vibrating micro cantilevers of tapping mode atomic force microscopy, Int. J. Non-Linear Mech. 42 (2007) 658–672.

[24] L. Zhou, Y. Chen, F. Chen, Global bifurcation analysis and chaos of an arch structure with parametric and forced excitation, Mech. Res. Commun. 37 (1) (2010) 67–71.

[25] Y. Shen, S. Yang, X. Liu, Nonlinear dynamics of a spur gear pair with time-varying stiffness and backlash based on incremental harmonic balance method, Int. J. Mech. Sci. 48 (2006) 1256–1263.

[26] Y.H. Guan, M. Li, T.C. Lim, W.S. Shepard Jr., Comparative analysis of actuator concept for active gear pair vibration control, J. Sound Vib. 269 (2004) 273–294.